

Universal Statistical Behavior of Neural Spike Trains

Naama Brenner,¹ Oded Agam,² William Bialek,¹ and Rob R. de Ruyter van Steveninck¹

¹NEC Research Institute, 4 Independence Way, Princeton, New Jersey 08540

²The Racah Institute of Physics, The Hebrew University, Jerusalem 91904, Israel

(Received 17 April 1998)

The statistical properties of spike trains generated by a sensory neuron are studied. It is shown that the spike trains exhibit universal statistical behavior over short times, modulated by a strongly stimulus-dependent behavior over long times. This decomposition is accounted for by a “frequency integrator” model, under conditions of time scale separation. We provide explicit formulas for the statistical properties in both the universal and the stimulus-dependent regimes, which are in very good agreement with the data. The universal regime is characterized by a dimensionless free parameter, which is observed experimentally to remain constant under different external stimuli. [S0031-9007(98)07566-8]

PACS numbers: 87.10.+e, 05.40.+j, 87.22.As, 84.35.+i

Neurons in the central nervous system communicate through the generation of stereotyped pulses, termed action potentials or spikes [1,2]. In many cases these spikes appear as a random sequence, even when external sensory stimuli are held constant. It is tempting to describe these responses in terms of stochastic models [3]. On the other hand, neurons in isolation are described quite accurately by microscopic, deterministic models of the form first proposed by Hodgkin and Huxley [4]. How do these microscopic dynamics relate to the observed statistics of spike trains? A crucial ingredient in making this link must be the properties of the noise that impinges upon the neuron, but little is known about the noise sources. Here we argue that, granting certain simple assumptions, a universal statistical behavior of spike sequences emerges on short time scales, independent of many poorly known details. The nonuniversal component of the response reflects the input signal and appears on longer time scales. These theoretical results are shown to be in good agreement with data from the fly visual system.

Many isolated neurons generate approximately regular sequences of spikes when injected a constant current [4–6]. The frequency of this firing is related to the value of the current by the nonlinear “ f/I curve.” Microscopic models aim in part at reproducing this curve correctly; simulations show that this is an essential ingredient for realistic spike train statistics in the presence of noise [7]. Rather than starting from a microscopic model, we take the f/I curve as a phenomenological description of the cell: when receiving an input s , a frequency $f(s)$ is determined, and a spike occurs when the time integral of this frequency completes a cycle. Noise from the environment, including photon shot noise and synaptic noise, is represented by a random function $n(t)$ added to the signal at the input (Fig. 1). The spike sequence is written as a train of Dirac δ functions, $\rho(t) = \sum_k \delta(t - t_k)$:

$$\rho(t) = \sum_k \delta(X(t) - k)\dot{X}(t), \quad (1)$$

where

$$X(t) = \int_0^t f[s(t') + n(t')] dt'. \quad (2)$$

This is closely related to the integrate-and-fire model [8]; we have introduced the non-negative function f to represent an underlying oscillator. For a constant input $s(t) = s$, the firing rate $r(s) = \langle \rho \rangle$ is related to the frequency response by

$$r(s) = \langle f(s + n) \rangle, \quad (3)$$

where $\langle \cdot \rangle$ denotes an average over noise. The firing rate is measurable experimentally as the average response to a repeated stimulus.

In our experiment, a live immobilized fly views various visual stimuli, chosen to excite the response of the cell H1. This large neuron is located several layers back from the eyes and receives input through connections to many other cells. It is identified as a motion detector, responding optimally to wide-field rigid horizontal motion, with strong direction selectivity [9]. The fly watches a screen with a random pattern of vertical dark and light bars, moving horizontally with a velocity $s(t)$. We record the electric signal of H1 from the vicinity of the cell and register a sequence of spike timings $\{t_k\}$ [10]. Figure 2 shows the time dependent firing rate $r(s(t))$ of H1 in response to a slow random signal $s(t)$, such that the relation (3) can be used locally in time. The plot of firing rate as a function of the instantaneous signal value (inset of Fig. 2), gives us $r(s)$, the noise smoothed version of $f(s)$.

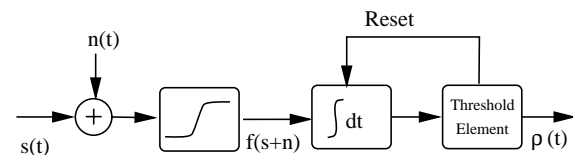


FIG. 1. Block diagram of the model for spike generation. The inputs are a signal $s(t)$ and a noise $n(t)$, which are added and passed through the frequency response function f . The frequency is integrated, and an action potential is generated when the integral completes a cycle.

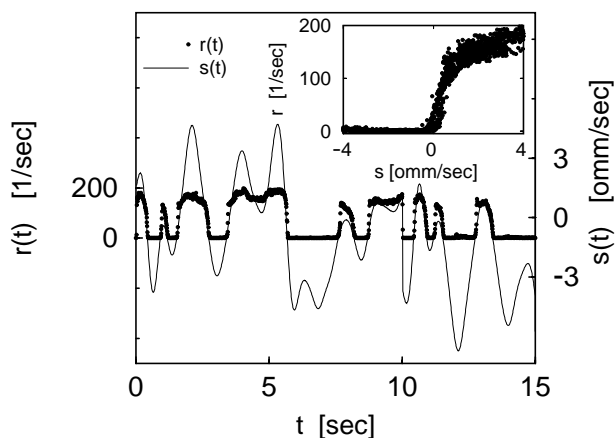


FIG. 2. Firing rate of H1 as a function of time, averaged over trials: $r(t) = \langle \rho(t) \rangle$ (dots), compared to the input signal $s(t)$ (solid line). We repeat the signal many times to obtain a sampling of the noise ensemble. The units of velocity are spacings of the compound eye's lattice (ommatidia) per sec. Inset: Instantaneous relation between r and s , which is a noise-smoothed version of the deterministic response $f(s)$.

The statistical structure of spike trains in the model of Eqs. (1) and (2) can be complicated, depending on the noise distribution $n(t)$ and the precise form of the function $f(s)$. However, universal behavior emerges if the stationary noise $n(t)$ is characterized by a correlation time, ξ_n , much shorter than the typical interspike interval, $1/r$. This implies that the integral in Eq. (2) is composed of a large number of statistically independent contributions and is therefore approximately Gaussian by the central limit theorem.

Consider first a constant input signal, $s(t) = s$. In this case, we obtain simple analytic formulas for the statistical properties of the spike trains. Figure 3 shows these theoretical results with the experimental data from the fly, for the interval distribution (Fig. 3a), the autocorrelation function (Fig. 3b), and the number variance (Fig. 3c). Data are shown in gray, and theory in solid black lines. All three characteristics depend on two parameters, one of which is the average firing rate $r(s) \equiv r$. Rescaling time to dimensionless units $\tau = rt$, we are left with one dimensionless parameter:

$$\gamma(s) = \xi_n \frac{\langle \delta f^2 \rangle}{\langle f \rangle}, \quad (4)$$

where $\langle f \rangle = \langle f(s + n) \rangle$, $\langle \delta f^2 \rangle = \langle f(s + n)^2 \rangle - \langle f(s + n) \rangle^2$, and ξ_n is the correlation time of the noise. γ measures the frequency modulation depth, and it will be shown to characterize the degree of irregularity in the resulting stochastic process.

The distribution of intervals between neighboring spikes $P(\tau)$ is the distribution of times where the oscillator completes a cycle. Assuming $\xi_n \ll 1/r$ we find (Fig. 3a)

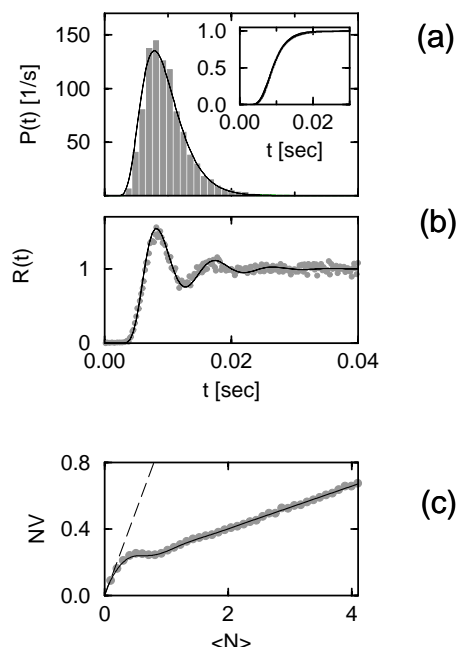


FIG. 3. Statistical properties of spike trains in the universal regime—experiment and theory. All data are taken from an experiment in which the fly watches dark and light bars forming a random pattern move across the screen with a constant angular velocity of 0.12 deg/sec. Fitting parameters are the overall spike rate and the irregularity parameter γ . (a) Probability distribution of the intervals between successive spikes. Histogram of intervals from the experiment (gray bars), and Eq. (5) (line). Inset: Fraction of intervals of length less than t (gray line) and integral of Eq. (5) (line). (b) Autocorrelation function calculated from the data (gray dots) and Eq. (6) (line). (c) Number variance as a function of number mean, as calculated from the data (gray dots) and Eq. (7) (line). For comparison, the number variance of a Poisson process is shown by a dashed line.

$$\begin{aligned} P(\tau) &= \frac{(1 + \tau)}{\sqrt{8\pi\gamma\tau^3}} e^{-[(\tau-1)^2/2\gamma\tau]} \\ &= \frac{d}{d\tau} \frac{1}{2} \left[1 + \operatorname{erf}\left(\frac{\tau-1}{\sqrt{2\gamma\tau}}\right) \right] \end{aligned} \quad (5)$$

[11]. The dimensionless parameter γ [defined by (4), with dependence on s suppressed], governs both the essential singularity at $\tau \rightarrow 0$ and the exponential decay at $\tau \rightarrow \infty$; it determines the coefficient of variation (ratio between standard deviation and mean) of the distribution and is therefore interpreted as an “irregularity parameter.” Equation (4) shows that the irregularity of the spike trains is determined both by the amplitude of the noise and by the sensitivity of the frequency function [7].

The symmetry between the two tails of the interval density takes the form of an exact invariance of the cumulative distribution: $F(\tau) = F(1/\tau)$. Starting from the measured intervals $\tau_k = t_{k+1} - t_k$, one may construct the dual point process with intervals $1/\tau_k$. Applying this transformation and plotting the two (scaled) distributions

reveals that the measured data indeed have this predicted invariance (Fig. 4).

The dimensionless autocorrelation function of the spike train, $R(\tau) = \langle \rho(0)\rho(\tau) \rangle / \langle \rho(0) \rangle^2$, is found to be (Fig. 3b)

$$R(\tau) = \delta(\tau) + \sum_{k \neq 0} \frac{(|\tau| + k)}{\sqrt{8\pi\gamma|\tau|^3}} e^{-[(|\tau|-k)^2/2\gamma|\tau|]}. \quad (6)$$

It is composed of an infinite sum of functions similar to the interval distribution, with shifted peaks. The number of peaks resolved is proportional to $1/\gamma$.

The number of spikes in a time interval of length τ is $N(\tau) = \int_0^\tau \rho(\tau') d\tau'$. It is a random variable, and its variance $NV = \langle \delta N^2 \rangle$ can be calculated under the same conditions (Fig. 3c):

$$NV = \gamma\tau + \sum_{m=1}^{\infty} \frac{1}{(m\pi)^2} [1 - \cos(2\pi m\tau)] e^{-2\pi^2 m^2 \gamma \tau}. \quad (7)$$

Here γ determines the slope of the asymptotic linear growth of the number variance [2]. For large γ , the “diffusion” in the number of spikes is higher, indicating again a more irregular behavior.

Data from two experiments with different constant stimuli were analyzed, and although the average firing rate varied, statistical properties agreed with the theory with similar values of γ .

How are the results for a constant stimulus relevant for the more natural case of dynamic stimuli? If $s(t)$ is slowly varying relative to $1/r$, it is expected that on short times the above results will hold, and slower modulations will appear on longer times. In our experiment, we control the velocity signal on the screen, but this signal passes several stages of processing in the visual pathway before arriving at the measured cell H1. The filtering of the incoming signal by photoreceptors and other elements render the effective signal arriving at H1 relatively slow and induce a natural separation of time scales between the effective signal and the spiking. Figures 5a–5c show the correlation functions of spike trains over short times from three experiments with different input signals: a

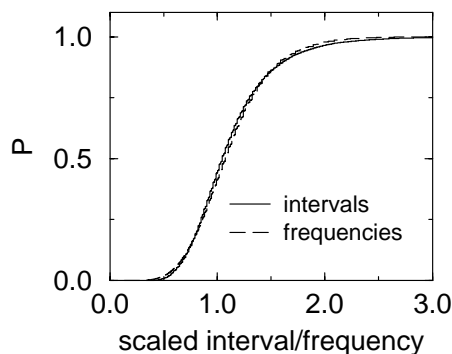


FIG. 4. The symmetry of the point process: distributions of normalized intervals τ and local frequencies $1/\tau$ are similar.

slow random signal, a sine, and a rapid random signal. These figures show that for $\tau < 2$ the behavior is similar to Fig. 3b. We call this the *universal regime*, since the statistical properties are largely independent of the input signal and are described by one parameter which is insensitive to many microscopic details of the neuron and of the noise. On longer times the curves begin to reflect correlations in the input signal (Figs. 5d–5f). Since these structures appear on times where the universal oscillations have already decayed, the two types of correlations decompose into a product:

$$R(\tau) \approx \frac{\overline{r(s(0))r(s(\tau))}}{r^2} \sum_{k \neq 0} \frac{(\tau + k)}{\sqrt{8\pi\gamma\tau^3}} e^{-[(\tau-k)^2/2\gamma\tau]}. \quad (8)$$

The term $\overline{r(s(0))r(s(\tau))}$ is the correlation function of the input signal, as seen through the noise-averaged response. In many cases, simple approximations give good fits to the long-time behavior. In Fig. 5f, a step approximation was used, giving rise to an exponential decay envelope typical of telegraph signals [12]. The exponent gives us the typical time scale of the filtered signal acting as the effective $s(t)$ in our model, about 20 ms in this experiment [2].

Since the irregularity γ is still a relevant parameter with dynamic stimuli (describing the behavior on short times), it is natural to ask how this parameter changes under different stimulus ensembles. We observe experimentally that in different ensembles of stationary signals, γ can be kept constant, although the mean firing rate r changes. Figure 6 shows that the correlation function from four experiments, with different types of input signal, overlap

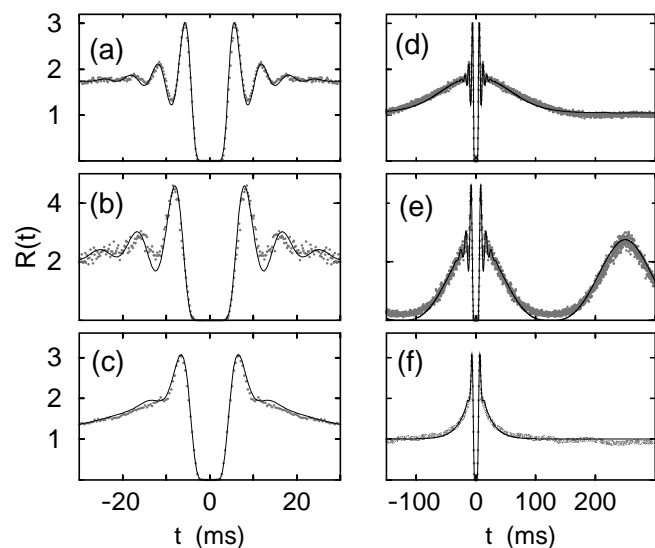


FIG. 5. Correlation functions of the spike trains over short times—the universal regime [(a)–(c)]; and over long times—the nonuniversal regime [(b)–(d)]. Data are shown in gray and theory [Eq. (8)], in black. (a),(d): random signal with a 5 Hz bandwidth; (b),(e): sine wave signal of period 0.25 sec; (c),(f): random signal with 250 Hz bandwidth.

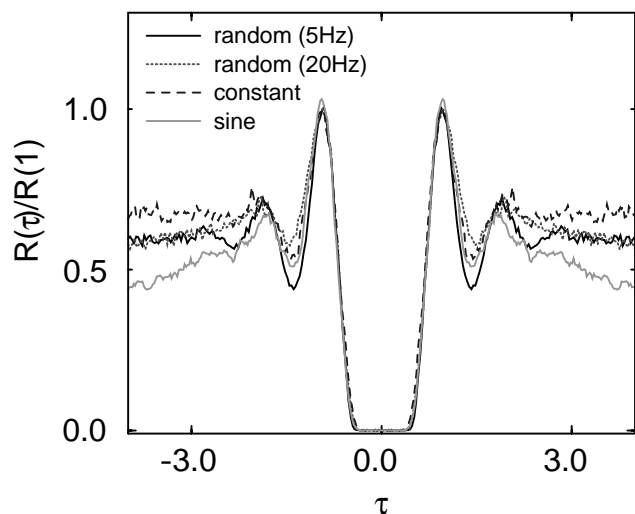


FIG. 6. Adaptation effects: correlation functions from experiments with different stimuli, plotted in dimensionless time units, are similar in the short time regime.

on short times. The figure is in dimensionless time units, so this overlap indicates a constant value of γ . Since γ is composed of the first two moments of f , and since the ensembles are varied by a different choice of signal, changes in the response function f must occur in order to keep γ constant. This has the simple interpretation of a gain control mechanism used by the system in adapting to different steady states, which is separate from the spike generating mechanism.

In conclusion, we have shown that a simple model predicts the statistical behavior of spike trains generated by a visual sensory neuron. Experiments were performed on a live fly, which was presented with a visual stimulus $s(t)$; the effect of the environment was modeled by a noise $n(t)$, and the response of the neuron was represented by a response function $f(s + n)$. The statistical properties of the spike trains are robust to the details of this response function as well as to the details of the noise. All these turn out to be described by one dimensionless parameter γ [see Eq. (4)], which depends on the first two moments of the $f(s + n)$. The spike trains exhibit universal statistical behavior over short time scales, independent of the input signal $s(t)$. On longer time scales the universal effects are attenuated by the noise, and the statistical properties of the spike trains are determined by input signal. These results are a consequence of a separation among the three basic time scales in the problem: the correlation time

of the noise ξ_n , the typical time for spiking $1/r$, and the correlation time of the input signal ξ_s ($\xi_n \ll 1/r \ll \xi_s$). The smallness of $\xi_n r$ is a phenomenological observation, whose consequences (formulas for the statistical properties at constant stimulus) are consistent with our data; it remains a challenge to give a microscopic explanation to this observation. The smallness of $1/\xi_s r$ is induced by filtering of the incoming motion signals in the photoreceptors and other stages of the visual pathway. We expect our results to be relevant also in other sensory neurons where the above conditions on the time scales hold. A higher degree of universality is observed as the system keeps the parameter γ fixed when external conditions are varied, so that the irregularity parameter characterized a given neuron under a set of conditions. This is a reflection of adaptational processes used to adjust to different steady states; relatively little is known about such processes.

Many thanks to G. Lewen for preparing the experiments and to N. Tishby and A. Schweitzer for comments.

-
- [1] D. J. Aidley, in *The Physiology of Excitable Cells*, edited by D. J. Aidley (Cambridge University Press, Cambridge, England, 1989).
 - [2] F. Rieke, D. Warland, R. de Ruyter van Steveninck, and W. Bialek, *Spikes: Exploring the Neural Code* (MIT Press, Cambridge, MA, 1997).
 - [3] A. V. Holden, *Models of the Stochastic Activity of Neurons*, Lecture Notes in Biomathematics (Springer-Verlag, Berlin, 1976).
 - [4] J. J. B. Jack, D. Noble, and R. W. Tsien, *Electric Current Flow in Excitable Cells* (Clarendon Press, Oxford, 1975).
 - [5] D. A. McCormick, B. W. Connors, B. W. Lighthall, and D. A. Prince, *J. Neurophysiol.* **54**, 782 (1985).
 - [6] Z. F. Mainen and T. J. Sejnowski, *Science* **268**, 1503 (1995).
 - [7] T. W. Troyer and K. D. Miller, *Neural. Comput.* **9**, 971 (1997).
 - [8] H. C. Tuckwell, *Introduction to Theoretical Neurobiology* (Cambridge University Press, Cambridge, England, 1988).
 - [9] K. Hausen and M. Egelhaaf, in *Facets of Vision*, edited by D. G. Stavenga and R. C. Hardie (Springer-Verlag, Berlin, 1989).
 - [10] For details, see R. de Ruyter van Steveninck and W. Bialek, *Philos. Trans. R. Soc. London B* **348**, 321 (1995).
 - [11] Equation (5) is similar, but not identical, to the first passage time of the Wiener process, G. L. Gerstein and B. Mandelbrot, *Biophys. J.* **4**, 41 (1964); see also [8] and K. Lindenberg *et al.*, *J. Stat. Phys.* **12**, 217 (1975).
 - [12] A more detailed account will be given elsewhere.